České vysoké učení technické v Praze
Fakulta jaderná a fyzikálně inženýrská

Czech Technical University Prague
Faculty of Nuclear Sciences and Physical Engineering

Ing. Hynek Lauschmann, CSc.

Aplikace metod analýzy obrazu ve fraktografii únavových lomů

Applications of image analysis methods in fractography of fatigue failures

SUMMARY

The reconstitution of the history of a fatigue crack growth is based on the knowledge of any correspondences between the morphology of crack surface and the velocity of crack growth (crack growth rate - CGR).

The traditional method utilizes striation patches - areas of striations, fine equidistant grooves in fracture surface. Striation patches may be recognized and evaluated by image analysis methods. A new definition of an ideal striation patch was necessary as a basis for an unambiguous algorithm. Two methods of automatical striation analysis were developed: a method based on recognition of single striation patches, and a method of direct estimation of mean striation parameters from the image as a whole.

The traditional approach cannot be applied when striations are not present or visible. For such cases, a new method - textural fractography - has been developed. Images of fracture surfaces are studied as image textures - "regularly random" image structures. The mezoscopic dimensional area with SEM magnifications between macro- and microfractography (about $30 \div 500$ x) is especially suitable. Pre-processing of images is necessary to obtain a homogeneous texture. Fractographic information is extracted in the form of integral parameters of whole images. Several methods of characterizing fractographic image textures have been investigated, tested and brought up to practical applicability: application of 2D Fourier transformation, modeling the texture as a Gibbs random field, and extraction and analysis of fibre-similar bright objects. Image parameters are related to the CGR by means of multilinear regression. Results of application on laboratory fatigue tests of stainless steel AISI 304L are shown.

Within fractography, image analysis methods open new possibilities of the acquisition of useful information from the morphology of fracture surfaces. Simultaneously, they save time of the operator and cost of the analyses by transferring the demanding manual work to the computer. The possibility of automatic extraction of the information from larger areas increases objectivity of the results.

In order to extract and analyze the fibre structure, special methods of image analysis have been developed - the method of tracing fibres and the database-oriented analysis of a fibre process.

SOUHRN

Rekonstrukce historie procesu růstu únavové trhliny vychází ze znalosti vzájemně jednoznačných vztahů mezi morfologií povrchu lomu a lokální makroskopickou rychlostí šíření trhliny (crack growth rate - CGR).

Tradiční metoda je založena na analýze polí striací - oblastí vyplněných striacemi, jemnými ekvidistantními žlábky v ploše lomu. Pole striací mohou být rozpoznávána a vyhodnocována metodami analýzy obrazu. Požadavek algorimizace postupu si vynutil formulovat novou, jednoznačnou definici ideálního pole striací. Byly vyvinuty dvě metody automatické analýzy striací - metoda založená na rozpoznávání jednotlivých polí striací a metoda odhadu průměrných striačních parametrů pro obraz jako celek..

Tradiční postup nemůže být aplikován, jestliže striace v lomové ploše nejsou, nebo nejsou viditelné. Pro tyto případy byla vyvinuta nová metoda - texturní fraktografie. Obrazy povrchu lomu jsou interpretovány jako obrazové textury - "pravidelně náhodné" obrazové struktury. Zvláště vhodná pro takový přístup jsou mezoskopická zvětšení řádkovacího elektronového mikroskopu mezi tradičními oblastmi makro- a mikrofraktografie (cca 30 ÷ 500 x). Obrazy je nutno předzpracovat, aby vyhodnocovaná textura byla homogenní. Fraktografická informace je vyjádřena integrálními parametry obrazu jako celku. Bylo studováno, testováno a k praktické aplikaci dovedeno několik metod vyjádření texturní obrazové informace vektorem číselných parametrů: aplikace 2D Fourierovy transformace, modelování textury jako Gibbsova náhodného pole a extrakce a analýza světlých objektů vláknové povahy. Vztah mezi obrazovými parametry a makroskopickou rychlostí šíření trhliny je vyjádřen formou multilineární regrese. Postup je dokumentován výsledky aplikace na lomové plochy vzorků z korozivzdorné oceli AISI 304L.

Aplikace metod analýzy obrazu ve fraktografii otevírá nové možnosti získávání informací o procesu lomu z lomových povrchů. Tyto metody současně převádějí většinu časově náročné rutinní práce na počítač. Tím šetří čas operátora a snižují náklady fraktografické analýzy. Možnost vyhodnotit automaticky informaci z větších ploch zvyšuje objektivitu výsledků.

V rámci rozpoznávání a analýzy obrazových vláknových struktur byly vyvinuty speciální postupy - metoda stopování vláken a databázově orientovaná analýza procesu vláken.

Keywords: database, fatigue, fibre process, Fourier transform, fractography, Gibbs random field, image texture, regression, striation.

Klíčová slova: databáze, Fourierova transformace, Gibbsovo náhodné pole, obrazová textura, proces vláken, regrese, striace, únava materiálu.

CONTENTS

1. INTRODUCTION

Fractography is an irreplaceable source of information on causes and mechanisms of fractures in practice. Traditional quantitative fractography acquired information especially from photographs of SEM views of crack surfaces. Evaluation of ***fractographic features*** - counting of them, measurement of their dimensions, distances, directions, etc., was done manually. Only strictly geometrically defined objects could be taken into account.

The progress of computers and image analysis methods inspired the development of the ***computer aided fractography***. Within the area of traditional information sources, it brings especially a more effective mode of the fractographic routine. Several applications will be discussed in chapter 2. However, application of image analysis opens up qualitatively new possibilities of the fractographic analysis. New sources of information can be used and new aspects of crack morphology studied. Several methods developed during recent years are described in chapter 3.

The basic task of the quantitative fractography of fatigue failures is the ***fractographic reconstitution of the history of a fatigue crack***, i.e., estimation of the dependence of the crack development (usually in the form of crack length a or of the cracked area) on the number N of loading cycles or blocks in the case of laboratory loading, or on the operational time of the structure. The main step [17,18] is estimation the course $v(a)$ of the ***crack growth rate (CGR)*** along crack length a. Then crack growth process $a(N)$ can be reconstituted by integration $\Delta N = \int \mathrm{d}a/v(a)$.

Specimens of the material are loaded in the laboratory under service conditions and the crack growth process is recorded. Fracture surfaces are documented by SEM and images are studied to relate some information present in the morphology of the crack surface to the macroscopic CGR. So a basis is obtained on which an unknown CGR can be estimated from the fracture surfaces of real parts.

2. APPLICATION OF IMAGE ANALYSIS IN TRADITIONAL FRACTOGRAPHY - ANALYSIS OF STRIATION PATCHES

2.1 Introductory notes

The traditional quantitative fractography of fatigue failures is based on striation patches (Fig.4, 5, 6) and/or beach lines. Striations are fine equidistant grooves in the fracture surface [4,17,18,19]. Striation spacing is the most valuable characteristic. The ratio between macroscopic CGR denoted v and the mean striation spacing $\overline{s}$ is a material function $D = v/\overline{s}$ [17,18]. From a known

$\overline{s}$, CGR can be estimated as $v = \overline{s}\ D(\overline{s})$.

Within this approach, image analysis methods can be used to ***recognize striations*** in images of crack surfaces, and to ***estimate their parameters***. A new definition of a striation patch linked closely to Fourier transformation will be discussed in sect. 2.2. Two methods of estimating striation parameters are described in sect. 2.3 and 2.4.

2.2 The new definition of an ideal striation patch

Traditionally, a striation patch is understood intuitively as a system of parallel strips. Striation vector ***s*** (spacing and direction) is measured along a perpendicular direction, which, in fact, is often more or less arbitrary (Fig.1a). If the plane of projection is not parallel to the plane of a striation patch, the angle relations are distorted, and the normal to striations in the image is different from the projection of the normal to striations in real space (Fig.1b). To understand the striation parameters unambiguously, let us define an ideal striation patch as a ***system of similar space arcs shifted equidistantly in the same direction*** [6]. Then vector of the shifting is the same in the whole patch (Fig.1c), and can be used to define the striation vector. Its projection is just the vector of the shifting of projected arcs (Fig.1d). Due to this, when following the above definition we are less subjective. Of course, real striation patches are not ideal. Assuming a model of the ideal striation patch, we estimate parameters of the idealization of the given striation patch towards the model.

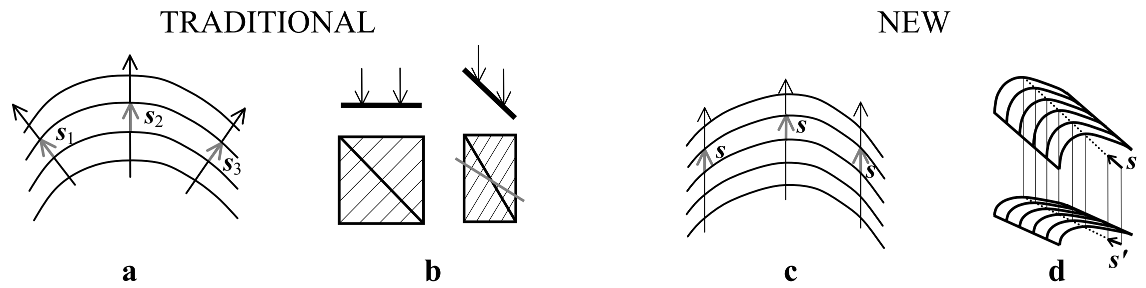

Fig.1: Traditional and new concept of a striation patch: **a** - the normal to arc striations is ambiguous, **b** - perpendicularity is distorted by projection, **c** - vector of shifting is unique in the whole patch, **d** - direction of shifting is invariant to projection.

The concept of shifting is closely related to the 2D Fourier transformation (FT). It consists in a decomposition of the image into planar waves. The spectrum of a system of straight striations contains one peak whose position determines the striation vector. The peak of a system of shifted arcs is linearly prolonged, and the shifting vector is related to its distance from the origin. The example of an application is shown in Fig.2. A striation patch in Al-2024 alloy has been scanned in three different positions. FT-based estimates of direction of striation vector (vector of shifting) are independent of the direction of observation.

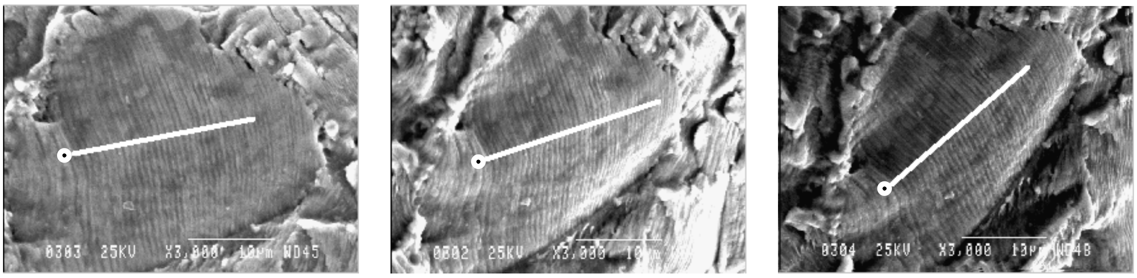

Fig.2: A striation patch recorded in different tilt. FT-based estimations of the direction of striation vector are the same in all cases.

2.3 The recognition of striation patches

The method is illustrated in Fig.3 [6]. After binarization, the presence of striations is tested in small subareas. Then neighbouring subareas are tested to create a striation patch. Finally, found patches are represented by rectangles, striation vectors estimated and visually presented to be verified by the operator.

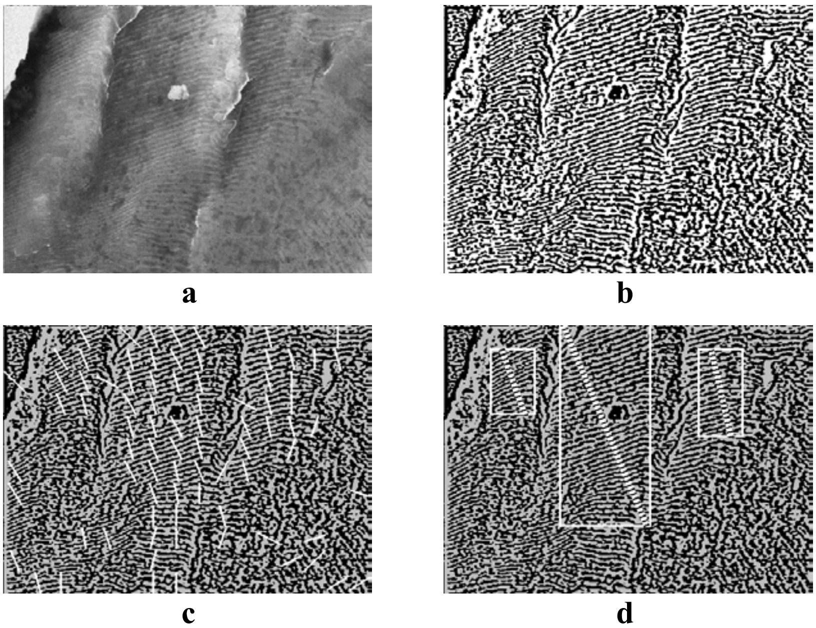

Fig.3: Recognition and analysis of striation patches: **a** - original image, **b** - binarization (filter Marr + median), **c** - local analysis of the presence of striations, **d** - joining rectangular areas representing striation patches, estimation the striation vectors.

2.4 Direct estimation of mean striation parameters

Usually mean striation parameters from a given area are used. They can be found [7] within one image directly from its spectrum (Fig.4). A single peak represents patches with similar striation vectors. The weight of peaks z_i can be expressed so that the mean striation vector can be estimated as $\overline{s} = \sum s_i z_i \Big/ \sum z_i$.

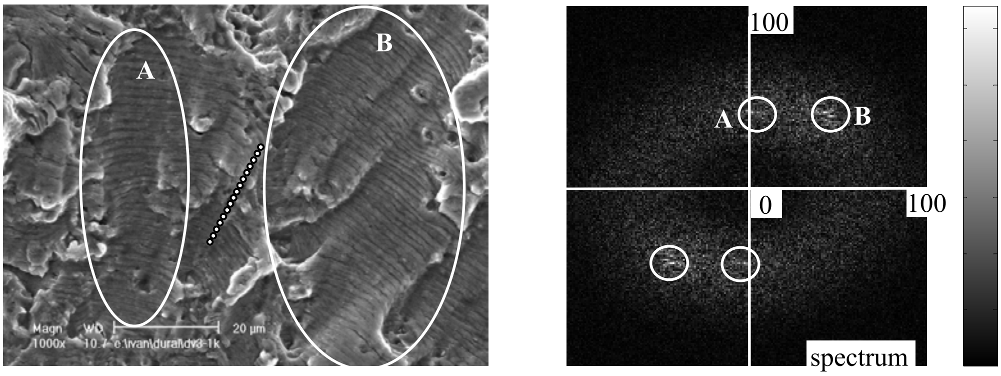

Fig.4: The original image, its Fourier spectrum with marked peak areas, and graphical representation of estimated mean striation vector.

3. TEXTURAL FRACTOGRAPHY

3.1 Introductory notes

Methods based on striations cannot be used when striations are not visible, typically due to corrosion [20,23]. As an alternative, a textural method has been developed in our department since about 1990. Structures in images of fracture surfaces are studied as image textures. The texture can be broadly defined as *a random structure of similar elements with some kind of ordering*. The main problem in fatigue fractography consists in mainly continuous brightness layout without distinct borders of textural elements.

Within the textural method, fractographic information is extracted in the form of numerical parameters of the whole image, ***integral fractographic characteristics***. Two general approaches to the analysis have been studied:

1. Estimation of statistical or model parameters directly from gray-scale images, without analysis of detailed geometrical structure. Two methods are shown, based on spectral characteristics (Fourier transformation, sect. 3.4.1) and gray-level coincidences (Gibbs random field model, sect. 3.4.2).
2. Extraction of textural elements followed by the application of binary random field analysis. A method aimed at fibre similar objects is described in sect. 3.4.3.

3.2 Setting SEM magnification

For the application of the textural method, the mezoscopic dimensional area with SEM magnifications between macro- and microfractography (about 30 to 500 x) is especially suitable. These magnifications were not used very much in the past for the absence of measurable objects in images. An appropriate magnification must be optimized with respect to following requirements:

Within one image: • the number of textural elements is representative, • the texture is approximately homogeneous (the change with increasing CGR is negligible), • the change of CGR within one image is negligible (CGR can be characterized by a constant).

Within the set of images: • the general character of all textures is the same (the same type of analysis can be applied), • some feature of the texture is significantly dependent on CGR.

Within the given image discretization: • textural elements supposed to be the source of information are well represented.

In practice, these requirements are counteracting and a compromise must be sought.

3.3 Pre-processing of images

Images must be pre-processed to obtain a homogeneous (transition invariant) texture, which is convenient for analysis. Significant fluctuations of mean brightness and contrast are often present in images and must be removed. These fluctuations are caused by morphological aspects (height and slope of crack surface) with characteristic dimensions corresponding to the image size or larger. A suitable method - normalization [8] - was derived by generalization from one-dimensional stochastic processes. Brightness is transformed by a moving algorithm to mean value 128 and standard deviation 50 (for an 8-bit range). In contrast to the generally used equalization [21], the shape of textural elements is conserved. The size of the mask is a very important parameter fundamentally affecting the results. A too small mask destroys textural elements to smaller ones, while a too large mask does not acquire the desired effect.

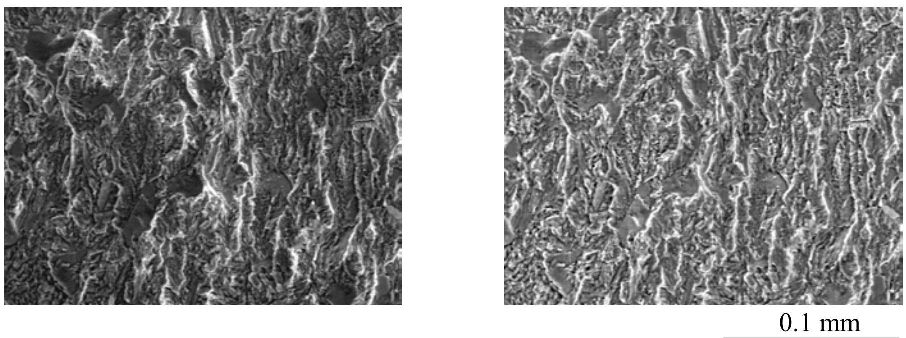

Fig.5: Original and normalized image (stainless steel AISI 304L).

3.4 Characterizing image texture - constructing a feature vector

The first step of fractographic textural analysis is characterizing each image of fracture surface by a set of numerical characteristics, a ***feature vector***. Several methods were investigated and developed up to practical applicability.

3.4.1 Spectral analysis

Single images of fracture surfaces are characterized by their spectrum. For the fractographic interpretation, suitable characteristics are not directional frequencies but distances and directions. That is why we interpret the spectrum in variables [period, direction] = $[p, \theta]$. In order to reduce the number of output spectral characteristics, a reasonable sorting of periods and directions can be introduced [9]. Single segments of the spectrum defined by the Cartesian product of period and direction intervals, $[p,\theta] \in (p_i, p_{i+1}) \times (\theta_j, \theta_{j+1})$, can be characterized by the mean spectrum

$$f_{i,j} = \sum_{r,s} a_{r,s}\delta_{r,s} \Big/ \sum_{r,s} \delta_{r,s} \;, \text{ where } \delta_{r,s} = \Big\langle \begin{array}{l} 1 \text{ if } p_{r,s} \in \langle p_i, p_{i+1}) \,,\; \theta_{r,s} \in \langle \theta_j, \theta_{j+1}) \;, \\ 0 \text{ otherwise} \,. \end{array} \tag{1}$$

For example, periods were classed into 15 intervals. The sorting of directions was limited to 3 classes: directions close to the direction of crack growth, directions close to crack front, and all other directions. All combinations created 45 segments, offering a feature vector of 45 components.

3.4.2 Gibbs random field model

A GRF model [3,11] of a texture is based on the term *pair interaction,* expressed in the simplest case by differences $d = x_1 - x_2$ between gray levels of two pixels. All pairs of pixels $[r,c]$ with the same distance vector $[i, j] = [r_1 - r_2, c_1 - c_2]$ create a clique. A list of cliques taken into account is called *search window* $\boldsymbol{W}$. At random textures, the significance of interactions decreases with the increasing distance between the pixels creating the pair.

The main sample characteristic of an image $\boldsymbol{X}$ is the gray level co-occurrence histogram $\boldsymbol{h}(\boldsymbol{X})$. $h_{i,j,d}$ is the number of interactions d in the clique $[i, j]$. Probability of interactions is $p_{i,j,d} = h_{i,j,d} / [(m-|i|)(n-|j|)]$, where m,n are image dimensions.

The main GRF characteristic is potential $\boldsymbol{V}$, a three-dimensional structure $\{V_{i,j,d}\}$ of the same size as $\boldsymbol{h}$. It compresses the information on gray level co-occurrences in the way similar to the energy of interactions of particles in statistical physics. Within a random field (space of images) defined by potential $\boldsymbol{V}$, two probability distributions are especially important:

Gibbs probability distribution of image $\boldsymbol{X}$ equals [3]

$$\Pr(\mathbf{X}) = \frac{\exp\big(\boldsymbol{V} * \boldsymbol{h}(\boldsymbol{X})\big)}{\sum_{\xi \in \Xi} \exp\big(\boldsymbol{V} * \boldsymbol{h}(\xi)\big)} \quad , \tag{2}$$

where * denotes a scalar product of arrays $\boldsymbol{V}$ and $\boldsymbol{h}(\boldsymbol{X})$ reshaped into vectors. The denominator is a normalization constant with Ξ denoting the set of all images.

The distribution of the probability of brightness in a pixel [*r,c*], given brightness values in all interacting pixels, is expressed by [3]

$$\Pr\left(x(r,c)\,\middle|\,x(r+i,c+j)\ ,[i,j]\in \boldsymbol{W}\setminus[0,0]\right)=\frac{\exp\sum\limits_{[i,j]\in\mathbf{W}\setminus[0,0]}\boldsymbol{V}_{i,j,x(r,c)-x(r+i,c+j)}}{\sum\limits_{u\in U}\exp\sum\limits_{[i,j]\in\mathbf{W}\setminus[0,0]}\boldsymbol{V}_{i,j,u-x(r+i,c+j)}}\ , \quad (3)$$

where U denotes the set of all possible values of brightness.

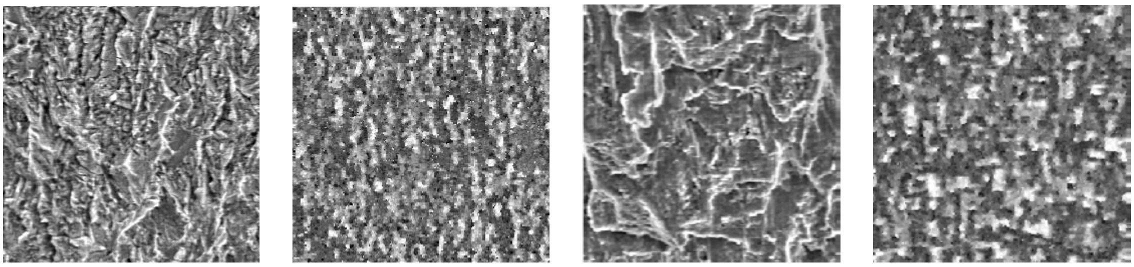

Fig.6: Comparison of original (a) and model (b) textures. Small (1) and high (2) CGR. Section 256 x 256 pixels.

For a given image $\boldsymbol{X_0}$, potential $\boldsymbol{V}$ can be estimated in two steps: The first approximation derived from the Taylor expansion of the likelihood function based on (2) is refined by means of stochastic relaxation using (3). In this way we obtain an estimate of the potential together with a model texture $\boldsymbol{X}^{(t)}$ which was optimized to be close to the image. In Fig.6, original and model textures are compared. Although visually the agreement is not very satisfactory, the final results are excellent.

A suitable measure of the significance of cliques [*i,j*] is their relative energies

$$e_{i,j}=\sum_{d\in D}V_{i,j,d}\ p_{i,j,d}(\boldsymbol{X_0})\,,\ [i,j]\in\boldsymbol{W}\,, \quad (4)$$

from which only those for small distance components *i,j* are significant. A set of significant relative energies reshaped into vector $\boldsymbol{f}$ can be used for the image feature vector.

3.4.3 Fibre process[1]

In many cases, the most remarkable elements of textures are light fibres with a different thickness and shape. They reflect sharp ridges and edges in the fracture surface. This structure can be abstracted into a fibre process [2,12], the properties of which are studied to find any sensitivity to CGR. The length of

[1] In stochastic geometry, the term *process* stands for a generalization of 1D stochastic processes (time series, etc.) to 2D or 3D definition set, defined by planar or spatial coordinates.

continuous fibres is an important property. The requirement to analyze the continuity of fibres in points of crossing or branching ("knots") made it necessary to create a database of the fibre process [13,15].

EXTRACTION OF FIBRES. The binarization of normalized images (Fig.7a) by threshold [2,8] met troubles because received objects did not correspond with qualities of fibres at any value of the threshold. A procedure, deliberately aimed at light fibre objects, was proposed in following steps [10,13]:

1. Fibre detection - Marr & Hildreth edge detection [21] modified on fibres (Fig.7b).
2. Tracing fibres. A successive procedure of replacing a thick fibre without distinct borders by a sequence of pixels (an analogy to skeleton, Fig.7c).

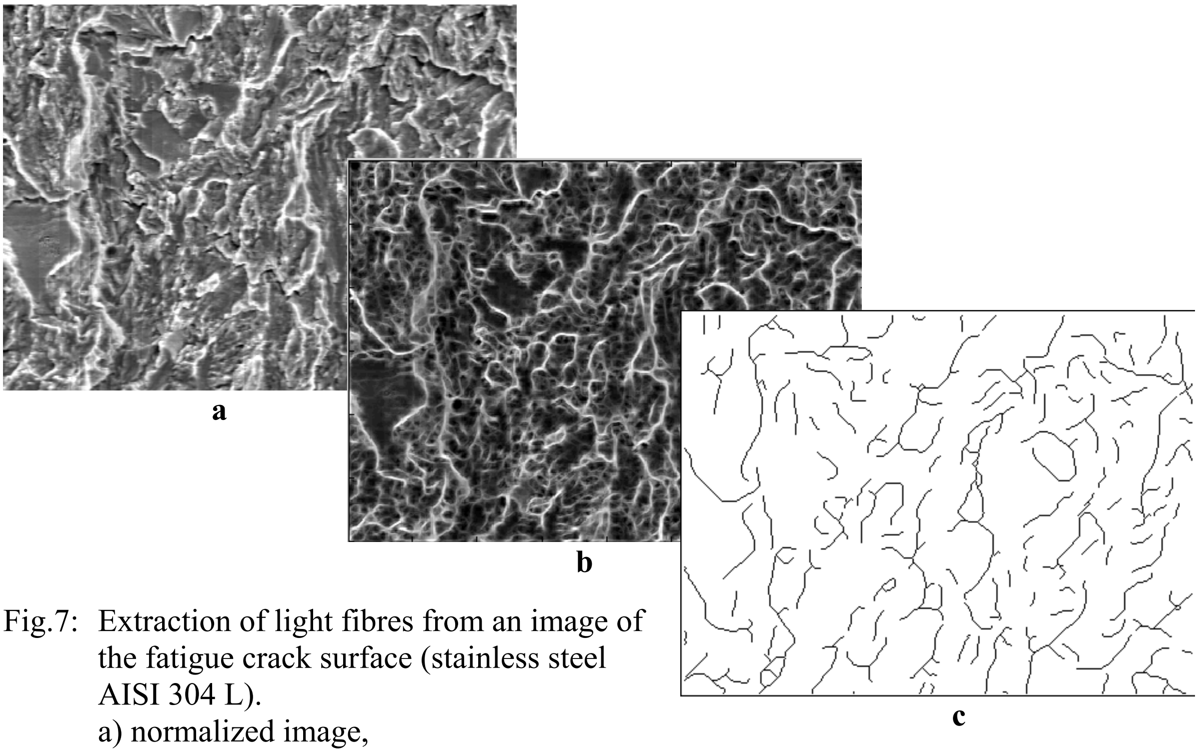

Fig.7: Extraction of light fibres from an image of the fatigue crack surface (stainless steel AISI 304 L).
a) normalized image,
b) fibre detection by $\boldsymbol{U}_{5,12}$ (rescaled into 8 bit range),
c) significant fibres traced.

FIBRE PROCESS ANALYSIS AND CREATION OF THE DATABASE [13,15]. For any description of a fibre process, the binarized image must be analyzed into elements: individual fibres, vertices and objects. Vertices are endpoints of fibres. Two types of vertices must be distinguished: isolated fibre endpoints and knots - common endpoints of several fibres. An object is a continuous set of fibres.

In order to classify pixels of the process as internal points, knots or endpoints, the number of changes *background - fibre* along a curve surrounding every pixel in a given distance can be used.

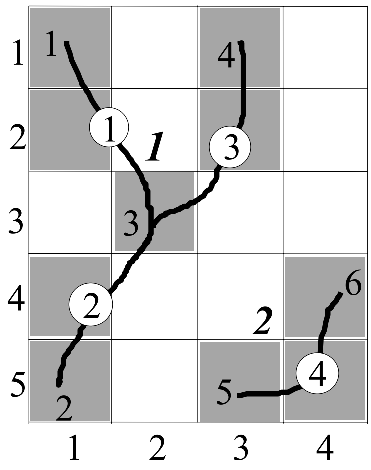

Objects: ***1,2*** $n_o = 2$

Fibres: 1 , 2 , 3 , 4 $n_f = 4$

Vertices: 1,2,3,4,5,6 $n_v = 6$

Pixels: $n_p = 10$

O - list of objects

the first vertex of the given object
$O(1) = 1$
$O(2) = 5$

V - list of vertices

	object	row	column	1/	2/
$V(1,:)$ =	[1	1	1	1	0]
$V(2,:)$ =	[1	5	1	2	0]
$V(3,:)$ =	[1	3	2	3	1]
$V(4,:)$ =	[1	1	3	0	3]
$V(5,:)$ =	[2	5	3	4	0]
$V(6,:)$ =	[2	4	4	0	4]

F - list of fibres

	vertex start	end	3/	4/
$F(1,:)$ =	[1	3	1	1]
$F(2,:)$ =	[2	3	2	2]
$F(3,:)$ =	[3	4	3	3]
$F(4,:)$ =	[5	6	4	4]

P - list of internal pixels of fibres

	row	column
$P(1,:)$ =	[2	1]
$P(2,:)$ =	[4	1]
$P(3,:)$ =	[2	3]
$P(4,:)$ =	[5	4]

[1]/The first fibre starting in the given vertex.
[2]/The first fibre on list $F(:,4)$, finishing in the given vertex.
[3]/The first internal pixel of the given fibre on list ***P***.
[4]/The list of fibres ordered by finishing vertex.

Fig.8: An example of a fibre process database

Single fibres are recorded from the starting to the finishing vertex. During the analysis, the database components are gradually filled in. The database structure was proposed so that it offers extracting information on objects and long fibres without browsing. An example of the database is shown in Fig.8.

PARAMETRIC MODEL AND JOINING LONG FIBRES IN KNOTS [13,15]. Let $[x_t, y_t]$, $t = 1,2,\ldots,n$ be the coordinates of fibre skeleton pixels in the sequence from the starting to the finishing vertex. A moving parametric regression can be used with the length of a single regression T and the shift of moving about $T/3$ (only the central third of the regression is accepted). For the regression function, we used a combination of the polynomial and polyharmonic models (corresponding to Taylor and Fourier decomposition) in the elementary form

$$\overline{x}(t) = a_{0j} + a_{1j}\tau + a_{2j}\sin(\varphi) + a_{3j}\sin(2\varphi) \ ,$$
$$\overline{y}(t) = b_{0j} + b_{1j}\tau + b_{2j}\sin(\varphi) + b_{3j}\sin(2\varphi) \ , \tag{5}$$
$$\text{where} \quad \tau = t - t_{0j} + 1, \ \ \varphi = \pi\tau / T \ .$$

Here j denotes the present recurrence of the regression and t_{0j} is its starting index. The linear component of functions (5) expresses the position and main course of the j-th segment, while the trigonometric components express its “waving”. A single regression does not have more than one inflection. In consequence, the maximum density of regression inflections is one for $T/3$ pixels of the fibre. This ratio defines the smoothing of details, which can be selected by setting T with respect to the aims of the analysis [10].

In every knot, all possible pairs of fibres are checked whether they create a longer fibre passing the knot. A common regression of merged fibres is estimated. If its curvature in the knot is smaller than a selected threshold, both fibres are judged as creating a passing one.

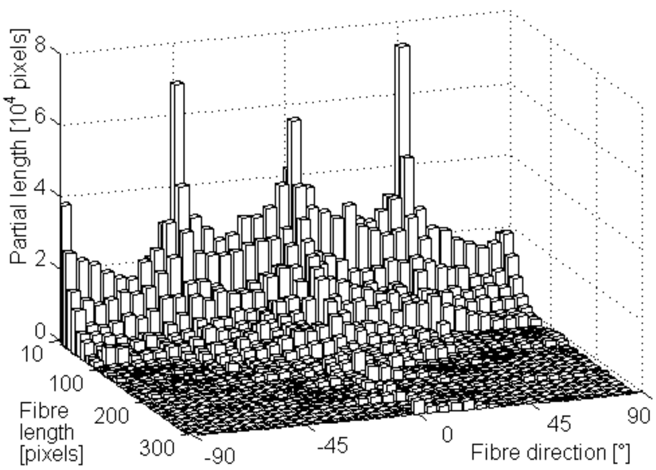

Fig.9: An example of the joint distribution of the lengths and orientations of light fibres from one image. 100 pixels ≈ 37.5 μm.

ESTIMATION OF FIBRE PROCESS CHARACTERISTICS [10,13]. The parametric model of a fibre process makes possible the estimation of a wide class of properties. Characteristics of length, direction, position and shape of fibres can be computed directly and exactly, without any problems with the discrete image representation. Also more complicated qualities can be studied - for example the joint distribution of lengths and orientations (Fig.9), the random process of the fibre orientation along its length, etc. Many of these characteristics would not be available by traditional methods.

For texture feature vector, the joint distribution of fibre length and orientation (Fig.9) was used. To lower the number of characteristics, sorting can be roughened (e.g. to four classes for the direction and six classes for the length, with resulting 24 image parameters).

3.5 Relating a feature vector and the crack growth rate - the multilinear model

Let us have a set of q images with assessed crack rates v_i , i=1,2,…,q, and characterized by a k-dimensional feature vector, i.e., a set of k textural parameters f_{iu} , u=1,2,…,k. The simplest model [9,12,15] expressing the CGR as a function of a set of image parameters is a multilinear function resulting into a system of regression equations

$$\overline{\log v_i} = \sum_{u=1}^{k} c_u f_{iu} + c_{k+1} \ , \ i = 1,2,...,q. \tag{6}$$

The set of parameters c_u can be estimated by the least squares method. The system must be strongly overdetermined - the number of equations (that matches the number of images) must be significantly greater then the number of estimated constants, $q>>k+1$.

Not all characteristics f_u predicate the CGR. Their significance can be proved by testing the zero value of the estimated coefficients c_u , u=1,…, k+1 [1]. We test the hypothesis H_0: $c_u = 0$ against the alternative H_1: $c_u \neq 0$. The test criterion is a Student's t-distributed statistic

$$t_u = c_u \left(\frac{\sum \left(\log v - \overline{\log v} \right)^2}{q-k-2} \left(\left(\boldsymbol{F}'\boldsymbol{F} \right)^{-1} \right)_{u,u} \right)^{-1/2} , \tag{7}$$

where $\boldsymbol{F}$ is a matrix with i-th row [f_{i1}, f_{i2}, ...,f_{ik}, 1]. If the absolute value of t_u is lower than the critical value at the selected level of significance α and q-k-2 degrees of freedom, $|t_u| < t_{1-\alpha/2}(q-k-2)$, hypothesis H_0 cannot be rejected and parameter f_u should be excluded.

A handicap originates from the multiparametric character of the method. The model counterbalances many increments from different sources of information. Therefore, a fractographic interpretation of the variety of textural elements is hardly possible.

3.6 Example of application

3.6.1 Experiment

Methods developed will be shown in an application to fatigue fracture surfaces of four laboratory specimens (C16 to C19) of stainless steel AISI 304L used in nuclear power plants [20]. CT specimens (Fig.10) were loaded by a constant triangular cycle with F_{min}=1450 N, F_{max} = 4850 N, f = 1 Hz in water at 20°C.

Fatigue crack surfaces were documented using SEM with magnification 200x (real image area 0.6 x 0.45 mm). The sequence of the images was located in the middle of the crack surface (Fig.10) and the images were distanced by 0.4 mm.

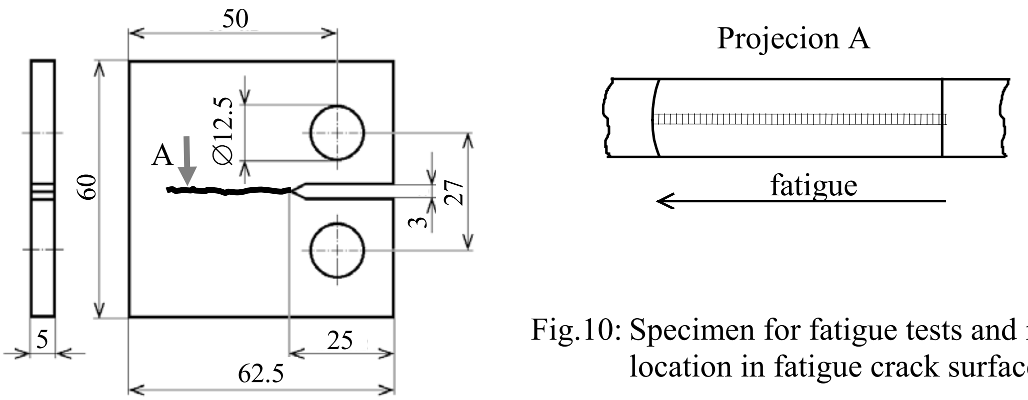

Fig.10: Specimen for fatigue tests and image location in fatigue crack surface.

A digital representation in 1200 x 1600 pixels and 256 brightness values was used. The total number of images was 165.

From frequently repeated records of the crack length the estimates of CGR were computed. The dependence of the CGR on crack length was estimated and every image was assessed a value of the CGR pertinent to its middle.

3.6.2 Typical results

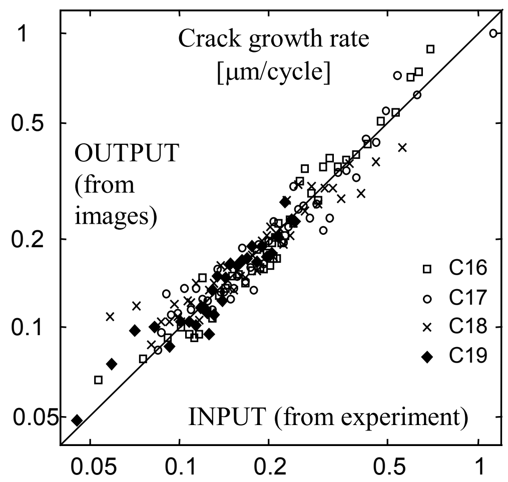

Fig.11: Comparison of crack rates taken for input and returned from spectrum of images of crack surfaces. Ideal agreement: $y = x$.

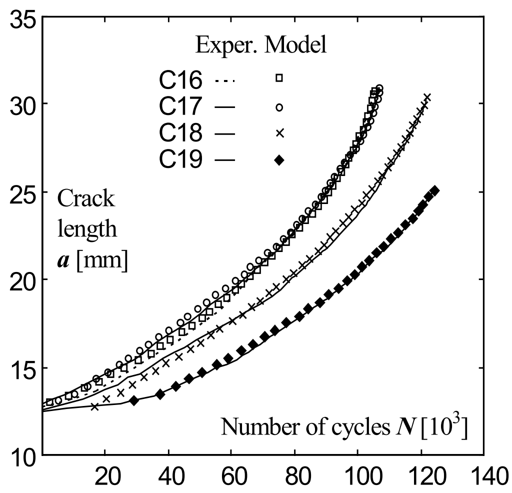

Fig.12: Crack growth in single specimens and reversal reconstitution (from the end to the origin) using crack rates estimated from images.

A comparison of experimental CGR taken for the input and CGR values returned from the images (while the spectral feature vector was used) is shown in Fig.11. The relations of crack length vs. the number of loading cycles are illustrated in Fig.12. One point represents one image. Results obtained with other methods are similar. The quality of results is fully satisfactory for practical application, and matches the best quality obtained by traditional method.

4. CONCLUSIONS

Within traditional fractography, the application of image analysis methods increases the volume and objectivity of acquired information.

Textural fractography can complement or substitute traditional methods. Simultaneously, it opens possibilities to extract new information from fracture surfaces, which has been concealed up to now.

Generally, image analysis methods save time of the operator and transfer the demanding routine work to the computer. The cost of analyses can be lowered and the reliability of results raised. The possibility of automatic extraction of the information from larger areas of fracture surfaces increases objectivity of the results.

Two new methods within the general frame of image analysis have been developed: The method of tracing fibres is a practical alternative to creating a skeleton for fibre structures without distinct borders in gray scale images. The database-oriented analysis of a fibre process offers a base for estimating useful characteristics, which were not accessible by traditional methods. The method was fully automated and could find a wide use in analyses of planar fibre processes, tessellations, etc.

The development of new methods of textural analysis for fractography continues (method of auto-shape decomposition [14], applications of wavelets [16], etc.). The next important stage of this research will be concerned with applications of image analysis in fractographic reconstitution of fatigue crack growth under variable cycle loading.

ACKNOWLEDGEMENT

This research has been supported by the Grant Agency of the Czech Republic, projects No. 106/97/0827 "Computer Aided Fractography" and 106/00/1715 "Computer aided quantitative fractography of fatigue failures".

REFERENCES

[1] Bakytová H., Hátle J., Novák I., Urgon M. (1986): Statistická indukce pro ekonomy. Praha – Bratislava, SNTL – Alfa, pp. 228–238.

[2] Čejka V., Beneš V. (1999): Computer Aided Fractography: Methods for evaluation of image anisotropy. In: Int. Conf. on Stereology, Spatial Statistics and Stochastic Geometry. Prague: Union of Czech Mathematicians and Physicists, pp. 89-94.

[3] Gimel'farb G.L. (1999): Image textures and Gibbs random fields. Dordrecht: Kluwer Academic Publishers, 250 p.

[4] Kunz J., Nedbal I., Siegl J., Pártl O. (1993): Fractographic Remarks to Fatigue Growth Rate. In: Proc. Fatigue '93 (Montreal). Vol.II, J.P.Bailon and I.J.Dickson, eds. Cradley Heath: EMAS, pp.649–654.

[5] Lauschmann H. (1997): Computer aided fractography. In: Proc.Int. Conf. Fractography '97. L.Parilák, ed. Košice: Institute of Materials Research of the Slovak Academy of Sciences, pp. 181-188.
[6] Lauschmann H. (1998): Computer Aided Fractography: The automatical evaluation of striation parameters. Engineering Mechanics No.6, Vol.5, pp. 377-380.
[7] Lauschmann H. (2000): Textural fractography: estimation of the mean striation spacing and direction. In: Int. Conf. on Stereology and Image Analysis in Materials Science. Eds. L. Wojnar & K. Rozniatowski. Cracow, Polish Society for Stereology, pp. 241-246.
[8] Lauschmann H. (2000): Textural analysis of fatigue crack surfaces - Image pre-processing. Acta Polytechnica Vol.40 No.4, Prague: CTU, pp. 123-129.
[9] Lauschmann H., Adámek J., Nedbal I. (2000): Textural fractography: Spectral analysis of images of fatigue crack surfaces. In: Fractography 2000. L. Parilák, ed. Košice: Institute of Materials Research of the Slovak Academy of Sciences, pp. 313-320.
[10] Lauschmann H., Wetzig K., Menzel S., Göbel T. (2001): Fractography of crack networks in thin layers. Materials Characterization 46, pp. 105-111.
[11] Lauschmann H., Ráček O. (2001): Textural fractography: Application of Gibbs random fields. In: Proc. 3rd Int. Conf. Materials Structure & Micromechanics of Fracture, Brno June 27-29, 2001. Brno University of Technology.
[12] Lauschmann H., Tůma M., Ráček O., Nedbal I. (2001): Textural fractography. 8th European Congress for Stereology & Image Analysis, Bordeaux Sept. 3-7, 2001. Image Analysis and Stereology; 20 (Suppl.1), pp. 372-378.
[13] Lauschmann H. (2001): A database-oriented analysis of a fibre process in fractography. 8th European Congress for Stereology & Image Analysis, Bordeaux Sept. 3-7, 2001. Image Analysis and Stereology; 20 (Suppl.1), pp. 379-385.
[14] Lauschmann H., Nedbal I. (2002): Auto-shape analysis of image textures in fractography. Image Analysis and Stereology, 2002, Vol.20, No.2, pp. 139-144.
[15] Lauschmann H., Tůma M., Ráček O., Nedbal I. (2002): Textural fractography. Image Analysis and Stereology, Vol. 21 Supl. 1, pp. S49-S59.
[16] Lauschmann H., Šumbera J., Nedbal I. (2003): Application of Wavelet Transform in Textural Fractography. In: Workshop 2003, CTU Prague (in print).
[17] Nedbal I., Siegl J., Kunz J. (1989): Relation Between Striation Spacing and Fatigue Crack Growth Rate in Al-Alloy Sheets. In: Advances in Fracture Research (Proc.ICF 7, Houston). K.Salama et al., eds. Vol. 5. Oxford: Pergamon Press, pp. 3483-3491.
[18] Nedbal I. et al. (1997): One lecture on fractography of fatigue failures. École d'Été - Dévelopments Récents en Fatigue des Matériaux et des Structures. Saint-Pierre d'Oléron, Juin 1997. Châtenay Malabry: École Centrale Paris - ICTM, 25 p.
[19] Nedbal I., Kunz J., Siegl J. (1997): Microfractographic Aspects of Fatigue Crack Growth in 7010 Aluminium Alloy. In: Proc.Int. Conf. Fractography '97. L.Parilák, ed. Košice: Institute of Materials Research of the Slovak Academy of Sciences, pp. 264-270.
[20] Nedbal I., Kunz J., Siegl J. (2000): Influence of corrosion environment and stress ratio on fatigue crack growth in stainless steel 304 L. In: Fractography 2000. L. Parilák, ed. Košice: Institute of Materials Research of the Slovak Academy of Sciences, pp. 293-300.
[21] Parker J.R. (1996): Algorithms for image processing and computer vision. John Wiley, New York, 417 p.
[22] Pratt W.K. (1978): Digital image processing. New York: John Wiley & Sons, pp. 235-242.
[23] Siegl J., Matocha K. (1997): Environmentally Assisted Cracking of 10GNN2MFA Low Alloy Steel. In: Proc. Int. Conf. Fractography '97. L.Parilák, ed. Košice: Institute of Materials Research of the Slovak Academy of Sciences, pp. 294–299.

ING. HYNEK LAUSCHMANN, CSc.

Born:	1955 in Prague
Professional career:	Czech Technical University Prague, Faculty of Nuclear Sciences and Physical Engineering (FNSPE), Department of Materials 1979 - M.Sc. 1985 - assistant researcher 1986 - Ph.D. 1988 - researcher 1994 - assistant professor 1999 - 2000 - 3-month visiting researcher at Institut für Festkörper- und Werkstofforschung, Dresden, Germany
Current position:	assistant professor, CTU Prague, FNSPE, Dept. of Materials
Membership in scientific societies:	International Society for Stereology Czech Society for Mechanics (member of comitee for Mechanics of Fatigue Failure of Materials) Czech Society for Cybernetics and Informatics
Research areas:	Probabilistic modeling of damage processes (till 1990) Computer aided fractography (since 1990), Textural fractography (since 1995) Experimental research of elastic properties and fatigue damage of materials, development of testing methods and instruments
Grant projects:	1997-1999 Computer aided fractography (Grant Agency of the Czech Republic, No. 106/97/0827) 2000-2002 Computer aided quantitative fractography of fatigue failures (Grant Agency of the Czech Republic, No.106/00/1715) 2003 Textural fractography of fatigue failures under variable cycle loading (Czech Technical University)
Lectures (in Czech):	Testing and processing of metals and alloys (since 1997) Failures I - Fatigue of metals (since 1997) Failures II (special lectures, since 1996) Project leader of 13 diploma theses
Applied research (cooperation, main items):	1986-89 Complex analysis of service loading of a locomotive axle, (FNSPE, ČKD Praha) 1992-94 Fatigue of Al-alloys for aircrafts Airbus (FNSPE, École Centrale Paris, Pechiney) 1996-02 Fatigue of stainless steel AISI 304 L (FNSPE, École Centrale Paris, Electricité de France)
Managing activities:	Building laboratories of the Dept. of Materials, FNSPE
Services:	Data analysis, image analysis, fatigue testing (within the team of the Dept. of Materials, FNSPE)